Contribution from the University Chemical Laboratory,
Cambridge University, Cambridge, CB2 1EW, U.K.

Ligand Fields from Misdirected Valency. 5. Consequences for Spectral Intensity Distributions

Melinda J. Duer and Malcolm Gerloch*

Received January 12, 1989

Cellular ligand-field energies in local C_s pseudosymmetry for a ligation in a metal complex characterized by bent bonding or other forms of misdirected valency require the off-diagonal cellular ligand-field (CLF) parameter $e_{\pi\sigma}$. The parametrization scheme required for the corresponding CLF intensity model is derived. It is shown that the effects of misdirected valency are primarily (and probably sufficiently) monitored through ${}^{L}t_{\sigma}$ and especially ${}^{L}t_{\pi}$ parameters. Detailed ligand-field analyses of both transition energies and intensity distributions in the "d-d" spectra of the five-coordinate Schiff-base complexes [bis(salicylidine-γ-aminopropyl)aminato]nickel(II) and [bis(salicylidene-γ-aminopropyl)methylaminato]nickel(II) are described. Discussions of optimal *e* and *t* parameter sets together furnish commentary upon the polarizations and lateral spreads of the electron distributions within the coordination bonds of these chromophores.

Introduction

The spatial subdivision of a ligand field that separates contributions between ligations and between bonding modes provides chemically comprehensible connections between d-electron properties and electron distributions in transition-metal complexes. Discriminations among bonding modes for local C_{2v} ligations is simply effected with the cellular ligand-field (CLF) parameter set (e_σ, $e_{\pi x}$, $e_{\pi y}$). Bent bonding or a significant role for a donor atom, nonbonding lone pair may define local C_s pseudosymmetry, however, and so requires[1-5] the additional, off-diagonal, parameter $e_{\pi\sigma}$. Neglect of the $e_{\pi\sigma}$ parameter will, at best, result in false optimal values for the remaining parameters: at worst, it will deny us reproduction of observed transition energies and other ligand-field properties. Its inclusion empowers the CLF method to define, in part at least, the nature of misdirected valency in object systems.

We recently developed[6-10] the ligand-field method to reproduce the relative *intensities* of "d-d" spectral transitions. Calculation of electric-dipole transition moments focuses upon the ligand-field wave functions whose d character has been established by prior CLF energy analysis. Intensity is deemed to arise from small admixtures of p and f character within those orbitals. We have defined a parameter scheme that reflects these characters and otherwise mirrors the superposition quality of the CLF energy parametrization. Analogous to the (e_λ; $\lambda = \sigma, \pi_x, \pi_y$) set we employ transition-moment parameters (${}^{L}t_\lambda$). The λ subscripts similarly label local bonding modes. The left superscript *L* takes, for the most part, values *P* and *F* according to whether the contribution to intensity ultimately derives from the p or f character in the local bond orbitals. This new approach to intensity modeling, which bears some formal relationship with that of Richardson and his group,[11-14] has been described quantitatively[6-8] and qualitatively.[9,10] We have begun to demonstrate how empirical ratios of ${}^{P}t_\lambda$ to ${}^{F}t_\lambda$ intensity parameters provide an interesting and powerful commentary upon the shapes of bond orbitals. The new model is applicable to acentric chromophores and has furnished quantitative reproduction of "d-d" intensity distributions in nearly a score of complexes to date. In its original formulation,[6] the approach considered ligations possessing local C_{2v} pseudosymmetry. In view of the extension of energy analyses to include misdirected valency in C_s symmetry, we now make an analogous extension to the intensity model. Theoretical considerations are followed by application to a closely related pair of formal trigonal-bipyramidal chromophores.

Theory

First, we show that while ${}^{L}t_{\pi\sigma}$ parameters, akin to $e_{\pi\sigma}$ for energies, are *not* required on lowering the local ligation pseudosymmetry from C_{2v} to C_s, many formal changes in the effective transition-moment operators do arise. Referring to the definitions of ${}^{L}t_\lambda$ parameters given in our original paper,[6] we recall, for C_{2v} symmetry, the expression of a local, or cellular, ligand-field oribtal as

$$\psi_\lambda = \mathrm{d}_\lambda + b_\lambda\phi_\lambda \qquad (1)$$

where $\lambda = \sigma, \pi_x$, or π_y and b_λ is a (small) mixing coefficient of all non-d orbitals of λ symmetry. Diagonal electric-dipole moments for the dipolar field oriented parallel to the local M-L vector (*z*) are given by

$$\begin{aligned} Q_z &= \langle\psi_\lambda|ez|\psi_\lambda\rangle \\ &= \langle\mathrm{d}_\lambda|ez|\mathrm{d}_\lambda\rangle && \mathrm{I} \\ &+ b[\langle\mathrm{d}_\lambda|ez|\phi_\lambda\rangle + \langle\phi_\lambda|ez|\mathrm{d}_\lambda\rangle] && \mathrm{II} \\ &+ b^2\langle\phi_\lambda|ez|\phi_\lambda\rangle && \mathrm{III} \end{aligned} \qquad (2)$$

Term I vanishes identically because of the parity rule. Terms II contribute only for those parts of ϕ that transform at the metal atom with p or f character, because of the selection rule $\Delta l = \pm 1$, and are parametrized by the quantities ${}^{P}t_\lambda$ and ${}^{F}t_\lambda$, respectively. Contributions from term III, parametrized with ${}^{R}t_\lambda$, tend to cancel in the global coordination geometries frequently possessed by typical chromophores.[6,8]

For the circumstances of misdirected valency in the *xz* plane and C_s symmetry, (1) is replaced by

$$\psi_\sigma = \mathrm{d}_{z^2} + a\mathrm{d}_{xz} + b\phi_\sigma + c\phi_{\pi x} \qquad (3)$$

$$\psi_{\pi x} = \mathrm{d}_{xz} + a'\mathrm{d}_{z^2} + c'\phi_\sigma + b'\phi_{\pi x} \qquad (4)$$

where ψ_σ represents that local cellular orbital which is predominantly d_{z^2}, and $\psi_{\pi x}$ that which is predominantly d_{xz}. The suffix labels σ and πx in (3) and (4) do not, of course, label irreducible representations of the C_s group. The contributions ϕ_σ and $\phi_{\pi x}$ are deemed to arise either from a misdirected "σ" ligand function or from the combination of an on-axis σ ligand function together with an off-axis lone pair. We will comment on likely relative magnitudes of the coefficients in (3) and (4) later.

(1) Deeth, R. J.; Duer, M. J.; Gerloch, M. *Inorg. Chem.* **1987**, *26*, 2573.
(2) Deeth, R. J.; Duer, M. J.; Gerloch, M. *Inorg. Chem.* **1987**, *26*, 2578.
(3) Deeth, R. J.; Gerloch, M. *Inorg. Chem.* **1987**, *26*, 2582.
(4) Fenton, N. D.; Gerloch, M. *Inorg. Chem.* **1987**, *26*, 3273.
(5) Fenton, N. D.; Gerloch, M. *Inorg. Chem.* **1989**, *28*, 2767.
(6) Brown, C. A.; Gerloch, M.; McMeeking, R. F. *Mol. Phys.* **1988**, *64*, 771.
(7) Brown, C. A.; Duer, M. J.; Gerloch, M.; McMeeking, R. F. *Mol. Phys.* **1988**, *64*, 793.
(8) Brown, C. A.; Duer, M. G.; Gerloch, M.; McMeeking, R. F. *Mol. Phys.* **1988**, *64*, 825.
(9) Fenton, N. D.; Gerloch, M. *Inorg. Chem.* **1989**, *28*, 2975.
(10) Duer, M. J.; Gerloch, M. *J. Chem. Soc., Dalton Trans.*, in press.
(11) Richardson, F. S.; Saxe, J. D.; Davis, S. A.; Faulkner, T. R. *Mol. Phys.* **1981**, *42*, 1401.
(12) Reid, M. F.; Dallara, J. J.; Richardson, F. S. *J. Chem. Phys.* **1983**, *79*, 5743.
(13) Reid, M. F.; Richardson, F. S. *J. Phys. Chem.* **1984**, *88*, 3579.
(14) May, P. S.; Reid, M. F.; Richardson, F. S. *Mol. Phys.* **1987**, *61*, 1471.

0020-1669/89/1328-4260$01.50/0

Expansion of electric-dipole transition moments is implemented as in (2) and section 3.2 of ref 6. For example

$$\langle\psi_\sigma|ez|\psi_\sigma\rangle = \langle d_{z^2}|ez|d_{z^2}\rangle + 2a\langle d_{z^2}|ez|d_{xz}\rangle + a^2\langle d_{xz}|ez|d_{xz}\rangle + 2b\langle d_{z^2}|ez|\phi_\sigma\rangle + 2ac\langle d_{xz}|ez|\phi_{\pi x}\rangle + b^2\langle\phi_\sigma|ez|\phi_\sigma\rangle + c^2\langle\phi_{\pi x}|ez|\phi_{\pi x}\rangle + 2c\langle d_{z^2}|ez|\phi_{\pi x}\rangle + 2ab\langle d_{xz}|ez|\phi_\sigma\rangle + 2bc\langle\phi_\sigma|ez|\phi_{\pi x}\rangle \quad (5)$$

The first three terms vanish identically because of the selection rule $\Delta l = \pm 1$ and the last two vanish because the angular part of the operator is diagonal. The third and fourth terms are related to the ${}^Lt_\sigma$ and ${}^Lt_{\pi x}$ parameters of the C_{2v} model. Using Table A3 of ref 6, we obtain

$$\langle\psi_\sigma|ez|\psi_\sigma\rangle = 2{}^Pt_\sigma + 2{}^Ft_\sigma + {}^Rt_\sigma + \frac{2ac}{b'}{}^Pt_{\pi x} + \frac{2ac}{b'}{}^Ft_{\pi x} + \frac{ac}{b'}{}^Rt_{\pi x} \quad (6)$$

Table V in Appendix A lists all similar matrix elements between ψ_σ and $\psi_{\pi x}$ under r_x and r_z. As discussed in sections 3.3 and 3.4 of ref 6, a central tactic in the ligand-field intensity model is the replacement of the odd electric-dipole operator, $e\mathbf{r}$, acting within ligand-field orbitals like (3), by even effective operators, $e\mathbf{T}$, acting within the d basis. Contributions to these effective transition moment operators, which arise additionally from misdirected valence, are calculated, as in ref 6, by using the general relationships between multipole expansion coefficients and matrix elements of one-electron operators given in Table 3.3 of ref 6. These extra contributions are listed in Table VI of Appendix A. We note that differences between operators for C_{2v} and C_s symmetry occur (a) by modification of previously nonzero multipole coefficients and (b) by replacement of previously zero coefficients by nonzero ones.

Algebraically, inclusion of misdirected valence within the intensity model introduces extensive changes. The extra contributions are still written in terms of the C_{2v}-type parameters ${}^Lt_\sigma$ and ${}^Lt_{\pi x}$ but with multipliers, α_i, related to the coefficients in (3) and (4). The α_i values, taken as

$$\alpha_1 = a \qquad \alpha_3 = c'/b \qquad \alpha_2 = a' \qquad \alpha_4 = c/b' \quad (7)$$

thus furnish a set of four new parameters to represent the effects of misdirected valency for any one ligand. At first sight, this extra parametrization seems too extensive for tractable analysis. Reasonable approximations, however, suggest a useful simplification.

Consider an approach to the functions in (3) and (4) in two stages. The off-axis nature of a bent bond or lone pair may be viewed as the addition of a π component to a primary σ bond. Within the overall C_s symmetry, we define basis functions

$$\sigma = d_{z^2} + \beta\phi_\sigma \qquad \pi = d_{xz} + \beta'\phi_{\pi x} \quad (8)$$

which directly recognize that π component. These functions mix to some extent under the local molecular Hamiltonian of C_s symmetry to yield ψ_σ and $\psi_{\pi x}$:

$$\psi_\sigma = d_{z^2} + \beta\phi_\sigma + \gamma(d_{xz} + \beta'\phi_{\pi x}) \quad (9)$$

$$\psi_{\pi x} = d_{xz} + \beta'\phi_{\pi x} + \gamma'(d_{z^2} + \beta\phi_\sigma) \quad (10)$$

Electric-dipole matrix elements arising from the first two terms in (9) or (10) are immediately of order ${}^Lt_\sigma$ or ${}^Lt_{\pi x}$, and so the most direct consequence of misdirected valency is to introduce nonzero ${}^Lt_\pi$ parameters where (for ligand σ donors) only zero values arise in C_{2v} geometry. Now we might reasonably suppose that the mixing coefficients β', γ, and γ' are of similar (small) magnitude. Then, nonzero contributions arising from the first with the fourth, or from the third with either the second or the fourth terms in (9) or (10) all occur to order ${}^Lt_\lambda$ times a mixing coefficient that is much less than unity. We therefore expect all these contributions to be secondary compared with the introduction of ${}^Lt_\pi$ (and associated decrease in ${}^Lt_\sigma$). It is further likely that the coefficients of $\phi_{\pi x}$ in (9) and of ϕ_σ in (10) will be smaller than all others.

In the analyses described below, we begin, therefore, with the "normal" C_{2v} parametrization scheme but with inclusion of ${}^Lt_{\pi x}$ parameters as first-order representatives of the misdirected valence.

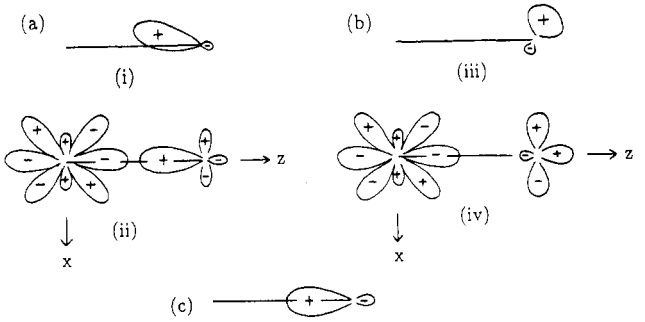

Figure 1. Orbital phasing (a) for bent bonds, (b) for "nonbonding" donor atom lone pairs, and (c) for "normal" σ bonding. The freely chosen phases in i and iii beget the component ligand function phases in ii and iv. The d-orbital phases in ii are determined by antibonding interactions with the ligand components. That of d_{xz} in iv is similarly determined by antibonding with the ligand π component: that of d_z2 in iv by antibonding with the (implicit) primary σ bonding as in part c.

These are followed, as detailed in Appendix B, with analyses that include all multipole components listed in Table VI with ranges of $|\alpha_i|$ up to 0.2: we guess that values greater than 0.1 are unrealistic anyway. The results in Appendix B suggest that the neglect of all modifications of the C_{2v} model other than the inclusion of ${}^Lt_{\pi x}$ contributions is satisfactory.

There now arises the question of the signs of contributions to ${}^Lt_\sigma$ and ${}^Lt_\pi$. We have shown elsewhere[8] that, like those of the e_λ parameters, these are determined by the donor or acceptor properties of the ligand in question. In C_{2v} symmetry, the signs of t parameters follow those of the corresponding e parameter. The circumstances of misdirected valency[1] are illustrated in Figure 1a for bent bonding and, in Figure 1b, for a "nonbonding" donor atom lone pair. The orbital phases i and iii are chosen freely. Those of the σ and π components of these ligand functions ii and iv then follow, as shown. Both forms of misdirected valency will be characterized by ligand donor roles. The consequent antibonding interaction with the metal d_σ and $d_{\pi x}$ orbitals establishes the metal orbital phasing in ii and so defines[8] positive ${}^Lt_\sigma$ and ${}^Lt_\pi$ parameters in this case. The phase of $d_{\pi x}$ in iv is similarly established with the same result for ${}^Lt_\pi$. However, the phase of d_σ in iv is determined by the overlain, "primary", ligand σ donation in part c. The sign of contributions to ${}^Lt_\sigma$ from the σ component of the ligand lone pair in iv is difficult to gauge, though, because of competing factors, as follows. The metal-directed lobe is bonding and will provide a negative contribution to ${}^Lt_\sigma$: the other lobe will make a positive contribution. The smaller, metal-directed, lobe lies in a region of larger d_σ amplitude, however, so there will be an overall tendency for cancellation. Prediction is further confused by the character of the integrals $\langle d|r|\phi\rangle$, which tend to emphasize the more outer parts of the ligation.[8]

Altogether, therefore, we expect the most visible results of misdirected valency for the intensity modeling to be monitored by positive ${}^Lt_\pi$ parameter values and only small, unpredictable contributions to ${}^Lt_\sigma$ variables.

Ligand-Field Analyses of Two 5-Coordinate Nickel(II) Chromophores

A. Energies. We present ligand-field analyses of the transition energies and intensity distributions for the five-coordinate, Schiff-base complexes [bis(salicylidene-γ-aminopropyl)methylaminato]nickel(II) and [bis(salicylidene-γ-aminopropyl)-aminato]nickel(II), abbreviated as Ni(salmedpt) and Ni(saldipa), respectively. X-ray structural analyses[15,16] show the crystal structures of these compounds as nonisomorphous, although the molecular complexes are closely isostructural, as summarized in Figure 2.

Calculations have been performed within the spin-triplet basis ${}^3F + {}^3P$, except for final refinement within the complete d^8 configuration, by using the CAMMAG2 program suite[17] developed

(15) Di Vaira, M.; Oroli, P. L.; Sacconi, L. *Inorg. Chem.* **1971**, *10*, 553.
(16) Seleborg, M.; Holt, S. L.; Post, B. *Inorg. Chem.* **1971**, *10*, 1501.

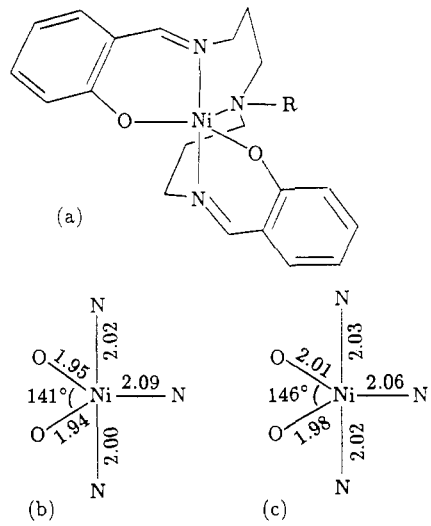

Figure 2. (a) Trigonal-bipyramidal coordination in Ni(salmedpt) and Ni(saldipa), R = CH_3 or H, respectively and (b) structural parameters in (b) Ni(salmedpt) and (c) Ni(saldipa).

Table I. Optimal Energy Parameters (cm^{-1}) That Reproduce Spectral Transition Energies in Ni(saldipa) and Ni(salmedpt)

param	Ni(saldipa)	Ni(salmedpt)[b]
e_σ(im)	5100	5100
$e_{\pi\perp}$(im)	0	0
e_σ(am)	3500	3300
e_σ(O)	4600	4000
$e_{\pi\perp}$(O)	1700	1100
$e_{\pi\parallel}$(O)	25	25
$e_{\pi\sigma}$(O)	900	1200
B	840	820
C	2700	3000
ζ[a]	450	450

[a] Not refined. [b] Values selected from the middle of a small correlated region of parameter space—see text.

in this laboratory. For each complex separately, the following parameters have been varied: for interelectron repulsion energies, the Racah B and C parameters; for the ligand field proper, the CLF parameters, e_σ(im), $e_{\pi\perp}$(im) for the Schiff base imines lying at the axial sites of the trigonal bipyramids, e_σ(am) for the equatorial amine, and e_σ, $e_{\pi\perp}$, $e_{\pi\parallel}$, and $e_{\pi\sigma}$ for the equatorial phenolic oxygen donors: $\parallel$ and $\perp$ refer to directions parallel and perpendicular to the salicylidene rings. The spin–orbit coupling coefficient, ζ, was held fixed at 450 cm^{-1}, throughout.

Single-crystal electronic spectra have been reported for each complex,[18] in a' and b polarization for Ni(salmedpt) and in b and c polarization for Ni(saldipa). Resolved features were noted in the range 7000–18 000 cm^{-1} together with a shoulder at ca. 21 000 cm^{-1} on intense charge-transfer transitions for Ni(saldipa). Earlier discussion[18,19] has been concerned with the question of which observed bands are to be assigned as components of $\rightarrow {}^3P$: the various suggested assignments were made without the benefit of quantitative support from modern analysis. In the present analyses, we have varied the CLF parameters throughout the following ranges: e_σ(any), 1500–6000 cm^{-1}; e_π(any), −2000 to +3500 cm^{-1}; $e_{\pi\sigma}$(O): = −1500 to +2500 cm^{-1}. We find that no combination of these parameters, with concomitant variations in B, will reproduce the observed band energies unless *all* spin-allowed transitions up to 18 000 cm^{-1} are assigned as components of the ${}^3F$ term. An essentially unique choice of parameter values reproduces the observed transition energies for Ni(saldipa): it is

Table II. Comparisons between Observed[18] Spin-Triplet[a] Transition Energies (cm^{-1}) and Those Calculated with the Optimal Parameter Sets of Table I

Ni(saldipa)		Ni(salmedpt)	
obsd	calcd	obsd	calcd
	27 155		26 074
	24 794		23 038
	23 476		22 355
17 300	17 140	17 300	16 369
14 000	14 581	13 900	14 228
	13 688	13 100	12 970
10 700	11 453	10 300	10 421
8 900	9 434	8 600	8 797
	3 361		1 948
	0		0

[a] The two lowest energy spin singlets are calculated to lie at 8225 and 11 735 cm^{-1} for Ni(saldipa) and at 7904 and 12 076 cm^{-1} for Ni(salmedpt). Observed spin-forbidden features are reported at 7800 and 11 700 cm^{-1} for Ni(saldipa) and at 11 800 cm^{-1} for Ni(salmedpt).

(salmedpt) is slightly less unique. Good fits occur within a small, extended region[21] of polyparameter space, values near the middle of which are listed in Table I. Of particular importance for the intensity analyses to follow, however, is the fact that the equivalent, global multipolar representation of the ligand field is essentially constant throughout this region of correlation. Thus, any small indeterminancy in the energy analysis does not carry over into the intensity analysis. Finally, comparisons between observed band energies and those calculated with the parameter sets of Table I are made in Table II.

B. Intensities. The axial imines in each complex are approximately centrosymmetrically related through the metal. Were this precise, contributions to intensities from these ligations would cancel exactly. The main departure from this lies in the inexact parallelism of the N=C bonds. We have therefore omitted ${}^Lt_\sigma$(im) parameters from the intensity analyses and only included ${}^Lt_{\pi\perp}$(im) toward the end of the process. In each case, contributions from this source were found to be trivial. In the following, therefore, we refer only to intensity parameters associated with the equatorial ligands: namely, ${}^Lt_\sigma$(am), ${}^Lt_\sigma$(O), ${}^Lt_{\pi\parallel}$(O) and ${}^Lt_{\pi\perp}$(O) for L = P, F, and R. However, contributions for L = R were found to be slight, partly due,[8] no doubt, to the triangular coordination. Apart from occasional trial calculations with nonzero ${}^Rt_\lambda$ parameters, the remainder of the analyses held all R contributions at zero. As discussed in the Theory section, all extra parameters, $\{\alpha\}$, were held at zero at this stage.

The relative intensities of the observed spectral bands were estimated by procedures described elsewhere.[7,9] For each molecule, with two polarizations reported, they provide a data base of eight intensities (seven relative). With the restrictions described above, these are to be reproduced with eight t parameters (seven relative), for each complex. The analyses proceed by systematic variation of all parameters in steps of 10 with respect to the largest (as determined by preliminary exploration) being held at 100 in the units of Table III, recording an agreement figure-of-merit based upon a minimum least-squares deviation. This wide, trial-and-error exploration of parameter space is always undertaken first in order not only to identify the region of regions of acceptable fit but also to establish any correlation between parameters affording good fit that would reveal any underdeterminancy in the analytical process. Final refinements of fits located in this way are conducted either by sampling on finer grids or, latterly, by standard least-squares algorithms. In this case, the intensity analysis for Ni(salmedpt) was straightforward, yielding an essentially unique parameter set to reproduce the observed intensity distribution quantitatively. This "t" parameter set is listed in Table III and

(17) "CAMMAG2", a FORTRAN computation suite by A. R. Dale, M. J. Duer, M. Gerloch, and R. F. McMeeking.
(18) Nemiroff, M.; Holt, S. L. *Inorg. Chem.* **1973**, *12*, 2032.
(19) Sacconi, L.; Bertini, I. *J. Am. Chem. Soc.* **1966**, *88*, 5180.
(20) Deeth, R. J.; Gerloch, M. *Inorg. Chem.* **1986**, *24*, 4490.
(21) Parameter values (cm^{-1}) at the limits of this linear correlation are as follows: e_σ(im) = 5000, $e_{\pi\perp}$(im) = 0, e_σ(am) = 3100, e_σ(O) = 4000, $e_{\pi\perp}$(O) = 1000, $e_{\pi\parallel}$(O) = 20, $e_{\pi\sigma}$(O) = 1000, B = 800; e_σ(im) = 5300, $e_{\pi\perp}$(im) = 400, e_σ(am) = 3500, e_σ(O) = 4000, $e_{\pi\perp}$(O) = 1100, $e_{\pi\parallel}$(O) = 20, $e_{\pi\sigma}$(O) = 1400, B = 840.

Table III. Relative Intensity Parameters (Arbitrary Units) for Ni(salmedpt)

param	$^{P}t_{\sigma}$(am)	$^{F}t_{\sigma}$(am)	$^{P}t_{\sigma}$(O)	$^{F}t_{\sigma}$(O)	$^{P}t_{\pi\perp}$(O)	$^{F}t_{\pi\perp}$(O)	$^{P}t_{\pi\parallel}$(O)	$^{F}t_{\pi\parallel}$(O)
value[a]	100 (20)	64 (15)	0 (20)	53 (25)	45 (5)	8 (25)	61 (20)	2 (25)

[a] Values in parentheses indicate parameter ranges affording acceptable reproduction of the observed intensity distribution.

Table IV. Comparisons between Observed[18] Relative Intensities[a] and Those Calculated with the Parameter Sets of Tables I and III for Ni(saldipa)[b] and Ni(salmedpt)

Ni(salmedpt)

energy range/ cm^{-1}	polarization a'		polarization b		average[c]	
	obsd	calcd	obsd	calcd	obsd	calcd
8 000–9 200	2	2	3	3	24	9
9 500–11 000	5	4	11	11		14
12 000–14 700	7	8	10	11	76	34
14 700–18 000	33	33	30	29		44

Ni(saldipa)[b]

energy range/ cm^{-1}	polarization b		polarization c		average[c]	
	obsd	calcd	obsd	calcd	obsd	calcd
8 000–9 500	14	12	5	2	30	14
9 500–12 000	5	4	5	10		14
12 500–15 000	5	22	6	4	70	27
15 000–18 500	39	11	21	35		45

[a] All intensities are expressed as percentages of the totals observed either for the crystals[18] or for solutions.[19] [b] Calculated values for Ni(saldipa) derive from the intensity parameter set for Ni(salmedpt) in Table III. [c] Average intensities are from solution spectra[19] and from the means of calculated intensities for light polarized parallel to a, b, and c.

the quality of fit is demonstrated in Table IV.

The intensity analysis for Ni(saldipa) failed utterly. Very wide variations of all equatorial P and F parameters were considered, and then with inclusion of $^{R}t_{\lambda}$ parameters, with inclusion of $^{L}t_{\lambda}$(im) parameters, and finally with variation of the spin–orbit coupling coefficient even though earlier experience[7] has suggested this to be remarkably unimportant. No acceptable reproduction of the reported intensity distribution was found. This is the only system studied by us to date to have been totally intractable. We do not believe the model to be at fault but rather the experimental data, for the following reasons.

Included in Table IV are intensities for Ni(saldipa) calculated with the optimal parameter set determined for Ni(salmedpt). While agreement with the intensity distribution for light reported as parallel to c might be acceptable, that for the b polarization is not. Also included in Table IV are corresponding comparisons, again using the parameter set of Table III throughout, for solution spectra reported by Sacconi and Bertini.[19] Although those solution spectra are not well resolved and would not provide satisfactory data on their own, agreement between theory and experiment is fair for both complexes. One is thus left in some doubt about the identification of the crystal axes and extinction directions in the Ni(saldipa) experiments and, we note here, the monoclinic class. Nemiroff and Holt[18] themselves were puzzled by the polarization ratios in Ni(saldipa) and concluded that an electronic symmetry close to D_{3h} with respect to the Ni–imine as principal axis was an appropriate description. This was to be contrasted with the proposed C_{2v} description favored for Ni(salmedpt). The true molecular symmetry for both compounds closely approximates C_2. Nemiroff and Holt expected these two complexes to be closely similar. The optimal CLF parameter values in Table I support that expectation.

Finally, we have examined the full contribution to intensities from misdirected valency by variation of the $\{\alpha\}$ of eq 7 above. These are detailed in Appendix B. In outline, the investigation began by computing the relative intensities resulting from the "best-fit" t parameters of Table III together with the supplementary contributions of Table VI for several sets of α values with $|\alpha_i| \leq 0.2$. Only modest changes of calculated intensity were observed for $|\alpha_i| \leq 0.1$ and even those for the surely unrealistic choice, $|\alpha_i| = 0.2$, were not gross. Then, for those same $\{\alpha\}$ sets,

Table V. Additional Nonzero Contributions to Electric-Dipole Matrix Elements for a Local Chromophore Symmetry Change from C_{2v} to C_s (Misdirected Valency in the xz Plane, Referred to (3) and (4))

$\langle\psi_{\sigma}|er_z|\psi_{\sigma}\rangle = 2(ac/b')^{P}t_{\pi x} + 2(ac/b')^{F}t_{\pi x}$

$\langle\psi_{\sigma}|er_x|\psi_{\sigma}\rangle = (1/3)^{1/2}[3a^{P}t_{\sigma} - 2(c/b')^{P}t_{\pi x}] + (1/3)^{1/2}[3(c/b')^{F}t_{\pi x} - 2a^{F}t_{\sigma}]$

$\langle\psi_{\pi x}|er_z|\psi_{\pi x}\rangle = 2(a'c'/b)^{P}t_{\sigma} + 2(a'c'/b)^{F}t_{\sigma}$

$\langle\psi_{\pi x}|er_x|\psi_{\pi x}\rangle = (1/3)^{1/2}[3(c'/b)^{P}t_{\sigma} - 2a'^{P}t_{\pi x}] + (1/3)^{1/2}[3a'^{F}t_{\pi x} - 2(c'/b)^{F}t_{\sigma}]$

$\langle\psi_{\pi x}|er_z|\psi_{\sigma}\rangle = ((c/b') + a)[^{P}t_{\pi x} + {}^{F}t_{\pi x}] + ((c'/b) + a')[^{P}t_{\sigma} + {}^{F}t_{\sigma}]$

$\langle\psi_{\pi x}|er_x|\psi_{\sigma}\rangle = (1/3)^{1/2}[(3/2)(1 + (ac'/b))^{P}t_{\sigma} - (1 + (a'c/b')^{P}t_{\pi x}] + (1/3)^{1/2}[(3/2)(1 + (a'c/b')^{F}t_{\pi x} - (1 + (ac'/b))^{F}t_{\sigma}]$

Table VI. Supplementary Nonzero Contributions to the Multipole Coefficients of Effective Transition-Moment Operators Arising from Misdirected Valency via Table V

(a) For $^{P}T_z$ and $^{F}T_z$

$c_{20} = c_{20}(C_{2v}) + 2(\pi/5)^{1/2}[2\alpha_1\alpha_4 t_{\pi x} + \alpha_2\alpha_3 t_{\sigma}]$

$c_{21} = c_{21}(C_{2v}) - (2\pi/5)^{1/2}[(\alpha_1 + \alpha_4)t_{\pi x} + (\alpha_2 + \alpha_3)t_{\sigma}]$

$c_{22} = c_{22}(C_{2v}) + 2(3\pi/10)^{1/2}\alpha_2\alpha_3 t_{\sigma}$

$c_{40} = c_{40}(C_{2v}) + (4/5)(\pi)^{1/2}[3\alpha_1\alpha_4 t_{\pi x} - 2\alpha_2\alpha_3 t_{\sigma}]$

$c_{41} = c_{41}(C_{2v}) - (12\pi/5)^{1/2}[(\alpha_1 + \alpha_4)t_{\pi x} + (\alpha_2 + \alpha_3)t_{\sigma}]$

$c_{42} = c_{42}(C_{2v}) + (24\pi/5)^{1/2}\alpha_2\alpha_3 t_{\sigma}$

(b) For $^{P}T_x$

$c_{20} = c_{20}(C_{2v}) + (\pi/15)^{1/2}[(6\alpha_1 + 3\alpha_3)^{P}t_{\sigma} - (2\alpha_2 + 4\alpha_4)^{P}t_{\pi x}]$

$c_{21} = c_{21}(C_{2v}) - (2\pi/5)^{1/2}[(3/2)\alpha_1\alpha_3{}^{P}t_{\sigma} - \alpha_2\alpha_4{}^{P}t_{\pi x}]$

$c_{22} = c_{22}(C_{2v}) + (\pi/10)^{1/2}[3\alpha_3{}^{P}t_{\sigma} - 2\alpha_2{}^{P}t_{\pi x}]$

$c_{40} = c_{40}(C_{2v}) + (4/5)(\pi/3)^{1/2}[((9/2)\alpha_1 - 3\alpha_3)^{P}t_{\sigma} + (2\alpha_2 - 3\alpha_4)^{P}t_{\pi x}]$

$c_{41} = c_{41}(C_{2v}) - (4\pi/5)^{1/2}[(3/2)\alpha_1\alpha_3{}^{P}t_{\sigma} - \alpha_2\alpha_4{}^{P}t_{\pi x}]$

$c_{42} = c_{42}(C_{2v}) + (2\pi/5)^{1/2}[3\alpha_3{}^{P}t_{\sigma} - 2\alpha_2{}^{P}t_{\pi x}]$

(c) For $^{F}T_x$

$c_{20} = c_{20}(C_{2v}) + (\pi/15)^{1/2}[(3\alpha_2 + 6\alpha_4)^{F}t_{\pi x} - (4\alpha_1 + 2\alpha_3)^{F}t_{\sigma}]$

$c_{21} = c_{21}(C_{2v}) - (2\pi/15)^{1/2}[(3/2)\alpha_2\alpha_4{}^{F}t_{\pi x} - \alpha_1\alpha_3{}^{F}t_{\sigma}]$

$c_{22} = c_{22}(C_{2v}) + (\pi/10)^{1/2}[3\alpha_2{}^{F}t_{\pi x} - 2\alpha_3{}^{F}t_{\sigma}]$

$c_{40} = c_{40}(C_{2v}) + (4/5)(\pi/3)^{1/2}[((9/2)\alpha_4 - 3\alpha_2)^{F}t_{\pi x} + (2\alpha_3 - 3\alpha_1)^{F}t_{\sigma}]$

$c_{41} = c_{41}(C_{2v}) - (4\pi/5)^{1/2}[(3/2)\alpha_2\alpha_4{}^{F}t_{\pi x} - \alpha_1\alpha_3{}^{F}t_{\sigma}]$

$c_{42} = c_{42}(C_{2v}) + (2\pi/5)^{1/2}[3\alpha_2{}^{F}t_{\pi x} - 2\alpha_3{}^{F}t_{\sigma}]$

all $^{L}t_{\lambda}$ values were optimized to best reproduce experiment. Changes of only 10–15 in $^{L}t_{\lambda}$ values relative to those in Table III were determined in this way, except for $^{F}t_{\pi\parallel}$(O). These parameters rapidly acquire negative values. It would be difficult to rationalize negative $^{L}t_{\pi\parallel}$ values throughout but the different signs of $^{P}t_{\pi\parallel}$ and $^{F}t_{\pi\parallel}$ surely characterize an unphysical parametrization.

As signaled earlier, our conclusions for the present study are that the effects of misdirected valency upon calculated intensities are adequately monitored through $e_{\pi\sigma}$ and $^{L}t_{\pi\parallel}$ parameters and that the more detailed changes summarized in Appendix A, which beget an intractable parametrization scheme, are of second order. Their neglect does not affect the quality of the discussion and correlation with chemical bonding that follows. We suspect that these conclusions are general, but we shall continue to check them in future analysis.

Discussion

Earlier applications of our intensity model have identified the ratios of P and F contributions as probes of bonding-electron distribution. Both theoretical[8] and empirical[8-10] arguments have been advanced to support the proposal that increased P contributions relative to F indicate bonds that are more polarized toward the metal or that are laterally more diffuse or both. We use the

Table VII. Effects upon Calculated Relative Intensities for Ni(salmedpt) for Various α Values[a]

	polarization *a'*					polarization *b*					polarization *c*				
band[a]	obsd	i[b]	ii[c]	iii[d]	iv[e]	obsd	i	ii	iii	iv	obsd	i	ii	iii	iv
1	2	2	2	1	1	3	3	3	3	3		9	10	9	9
2	5	4	6	7	7	11	11	5	2	2		8	7	7	7
3	7	8	9	10	10	10	11	9	8	8		37	32	27	27
4	33	33	41	47	47	30	29	26	22	22		12	11	9	10

[a] Band numbers correspond, in order, to the energy ranges given in Table IV. [b] i: ${}^{L}t_{\lambda}$ parameter set of Table III with $\alpha_1 = \alpha_2 = \alpha_3 = \alpha_4 = 0.00$. [c] ii: as for i but with $\alpha_1 = \alpha_2 = \alpha_3 = \alpha_4 = 0.05$. [d] iii: as for i but with $\alpha_1 = \alpha_2 = \alpha_3 = \alpha_4 = 0.10$. [e] iv: as for i but with $\alpha_1 = \alpha_2 = 0.20$ and $\alpha_3 = \alpha_4 = 0.00$.

Table VIII. Optimal ${}^{L}t_{\lambda}$ Parameter Values, Affording Quantitative Reproduction of Experimental Intensities for Ni(salmedpt) for the Same Sets of α Parameters Quoted in Table VII

α set	${}^{P}t_{\sigma}$(am)[a]	${}^{F}t_{\sigma}$(am)	${}^{P}t_{\sigma}$(O)[a]	${}^{F}t_{\sigma}$(O)	${}^{P}t_{\pi\perp}$(O)	${}^{F}t_{\pi\perp}$(O)	${}^{P}t_{\pi\parallel}$(O)	${}^{F}t_{\pi\parallel}$(O)
i	100	64	0	53	45	8	61	2
ii	100	61	0	43	38	−2	53	−23
iii	100	55	0	38	35	−5	47	−37
iv	100	52	0	41	33	−1	46	−39

[a] Fixed values.

present Theory section and wider experience of the CLF *e* parameterization to comment on each of the metal–ligand interactions in Ni(salmedpt).

Nonbonding Oxygen Lone Pairs. The positive sign found for $e_{\pi\sigma}$(O) places off-axis perturbation in the Ni–O ligation in the negative quadrant[1] of Figure 1 and so reflects the role of the nonbonding density of the oxygen lone pair. The significant magnitude of $e_{\pi\sigma}$(O) together with the very small value of $e_{\pi\parallel}$(O) accord with this conclusion (a) by virtue of the lesser overlap expected with d_{xz} and (b) by comparison with similar magnitudes observed for lone-pair perturbations.[1,2] The misdirected valency is also evidenced strongly by the relative magnitude of the ${}^{P}t_{\pi\parallel}$(O) intensity parameter. That the *P* contribution so overwhelms the *F* cannot be understood in terms of a strong polarization toward the metal but rather in terms of a relatively wide lateral spread[10] of the lone pair that would agree well with its expected diffuseness. Finally, the important role of the off-axis function for intensities as compared with energies is no cause for concern. As discussed elsewhere,[8] integrals of the form $\langle d|r|\phi\rangle$ emphasise those parts of the local environment which are more distant from the metal as compared with the energy integrals having the form $\langle d|V|\phi\rangle$.

M–L σ Bonding. The e_{σ} parameters describe M–L σ bonding that decreases along the series imine > oxygen > amine. The much larger value for the imine ligations is quite typical of the axial fields found[20] in other trigonal-bipyramidal complexes of nickel(II) and copper(II). It arises from the greater d-electron density in the equatorial plane than along the principal axis, together with the demands of the electroneutrality principle, as discussed in full elsewhere.[20] The larger fields of the phenolic oxygen ligations relative to that of the amine, on the other hand, presumably reflect a greater electron donation from the formally negatively charged oxygen donor. As that charge leaves the oxygen atom, it concentrates more strongly on the internuclear axis. The relative compactness of the Ni–O bond over the Ni–amine bond is reflected in the greater ${}^{F}t_{\sigma}/{}^{P}t_{\sigma}$ ratio in the former, determined from the intensity analysis. Similar qualities characterize the Co–O and Co–N bonds in a recent study of CoO_2S_2 and CoN_2S_2 chromophores.[10]

Ni–O $\pi_{\perp}$ Bonding. The Schiff-base oxygens act as both σ and π donors as expected and as revealed by several earlier ligand-field analyses. The smaller ratio ${}^{P}t_{\pi\perp}(O)/{}^{F}t_{\pi\perp}(O)$ relative to ${}^{P}t_{\pi\parallel}(O)/{}^{F}t_{\pi\parallel}(O)$ suggests that the "normal" bond orbital is laterally less diffuse than the lone pair.

Ni–Imine $\pi_{\perp}$ Bonding. The energy analysis indicates a negligible π-donor role for the axial imine groups. We account for this in terms of the consequences of the steric role of the d shell. First, the d_{xz} and d_{yz} orbitals (referred to *z* as the "3-fold" axis of the trigonal-bipyramidal coordination) are full and so tend to oppose donation from the axial ligands. Second, and probably more significant, is that the d configuration that facilitated strong axial σ donation inevitably frustrates π donation from the same ligands because of their requirement to achieve electroneutrality.

Acknowledgment. We thank Neil D. Fenton for helpful discussions and record the award of an SERC Research Studentship to M.J.D.

Appendix A

In Table V are listed supplementary contributions to Table A3 of ref 6 to model the effects of misdirected valence with reference to the cellular ligand-field orbitals of eq 3 and 4. No contributions involving ${}^{R}t_{\lambda}$ parameters are included for the following reasons: (a) as in ref. 6, contributions to transition moments perpendicular to the local *z* direction are deemed negligible (see Appendix 2 of ref 6), and (b) in ref 8, it was demonstrated that *R* type contributions in molecules with bipyramidal or antiprismatic symmetry cancel overall. In ref 8–10, it was further shown that these contributions are unimportant for chromophores whose global geometry approaches these ideals.

Then, in terms of the $\{\alpha\}$ of eq 7, we construct additional contributions to the effective transition-moment operators, as in Table VI (cf. Table 3.5 of ref 6).

Appendix B

Here, we report analyses of the intensity distributions in Ni(salmedpt) based upon the "best-fit" parameters of Table III but with inclusion of the supplementary contributions listed in Appendix A and parametrized with the $\{\alpha\}$ of eq 7.

First, in Table VII we present calculated intensities for $|\alpha_i| \leq 0.2$ with the ${}^{L}t_{\lambda}$ parameters of Table III. Then, in Table VIII, we list optimal ${}^{L}t_{\lambda}$ parameters for the same choices of $\{\alpha\}$ derived by least-squares fitting procedures. In each case, the agreement between observed and calculated relative intensities is no worse than that shown in Table IV. Calculations similar to those reported in Tables VII and VIII were performed for intermediate values of α_i, for example with $\alpha_1 = \alpha_2 = 0.1$ and $\alpha_3 = \alpha_4 = 0.0$. In each case, broadly similar results were obtained.